INTERNATIONAL JOURNAL OF PRECISION ENGINEERING AND MANUFACTURING Vol. 14, No. 10, pp. 1839-1846

DOI: 10.1007/s12541-013-0246-0

Analysis of Squareness Measurement using a Laser Interferometer System

Dong-Mok Lee[1], Hoon-Hee Lee[2], and Seung-Han Yang[2,#]

1 Institute of Mechanical Engineering Technology, Kyungpook National University, 80 Daehak-ro, Buk-gu, Daegu, Republic of Korea, 702-701
2 School of Mechanical Engineering, Kyungpook National University, 80 Daehak-ro, Buk-gu, Daegu, Republic of Korea, 702-701
Corresponding Author / E-mail: syang@knu.ac.kr, TEL: +82-53-950-6569, FAX: +82-53-950-6650

KEYWORDS: Squareness measurement, Laser interferometer, Abbe's error, Representative line, Best fit, Optical square

Squareness measurements of the driving axes of a machine tool are very important in order to evaluate the performance of the machine. A laser interferometer measurement is one of the most reliable ways to measure squareness. However, a squareness measurement using a laser interferometer system with an optical square causes restrictions in the straightness interferometer setup, which results in the occurrence of Abbe's offset. The Abbe's offset combined with angular errors during the motion of an axis causes Abbe's error. In addition, difficulty in the optical square setup causes restrictions on other optics and limitations of the measurable range. We present mathematical approaches that can be used to eliminate Abbe's error and to estimate squareness over the full range by using the best fit of straightness data measured without an optical square. Experiments for squareness measurements of a three-axis machine tool are conducted. The proposed techniques are used for squareness evaluation with the elimination of Abbe's error and also for squareness estimation for the full travel range.

Manuscript received: December 13, 2012 / Accepted: July 23, 2013

NOMENCLATURE

a_{ij} = Abbe's offset in i-direction of j-axis

e_{ij} = Abbe's error in i-direction of j-axis

r_{ij} = straightness data measured with Abbe's offset in i-direction of j-axis, $i=x, y, z; j=x, y, z$

m_{ij} = straightness data with Abbe's error eliminated from r_{ij} in i-direction of j-axis, $i=x, y, z; j=x, y, z$

ε_{ij} = angular error in i-direction of j-axis, $i=x, y, z; j=x, y, z$

s_{ij}, s_{ij}' = squareness of ij-plane for measurable and full travel range, respectively

δ_{ij} = straightness error in i-direction of j-axis, $i=x, y, z; j=x, y, z$

α, β = inclination of representative line of measurement data from the X-axis and Y-axis, respectively

$\Delta\alpha, \Delta\beta$ = difference in inclination of straightness representative lines for measurements with and without optical square at X-axis and Y-axis, respectively

α', β' = inclination of straightness representative line (best fit curve) from X-axis and Y-axis, respectively

1. Introduction

Geometric errors of a machine tool are one of the primary error sources affecting the positioning accuracy of a feed system. These errors can be measured by indirect methods such as position sensing detector (PSD), capacitive sensor, and double ball-bar (DBB) system, and by direct methods such as laser interferometer measurement system.[1-8] Among these geometric errors, the volumetric error is affected significantly by squareness, which is difficult to measure and analyze.[9] In the ISO 230 standard, squareness measurement techniques are introduced using a combination of a master square, dial gauge, micrometer, laser interferometer, and other components.[10] Lee[11] suggested a squareness measurement using an inexpensive master square and vision system since the production of a master square is difficult, and measurements using a laser interferometer involve more measuring time and higher equipment cost. To estimate the squareness, Yuan suggested an analysis algorithm with reverse kinematics using DBB circular test data.[12] A method of multi-degree of freedom measurement using capacitance sensors was suggested by Lee.[13,14] Laser interferometer systems are widely used to measure geometric error.[15,16] Consequently, major equipment manufacturers such as Renishaw plc and Agilent have developed optical square for squareness measurements.[17,18]

In order to reduce measurement uncertainty, geometric error measurement using a laser interferometer has been performed under conditions where the cosine error and Abbe's error are minimized.[19,20] Guidance is provided by many equipment manufacturers regarding data processing methods to eliminate measurement uncertainty. These considerations are especially important during squareness measurements. However, due to misalignment between the laser beam and the direction of feed, and also limitations in the optics setup, this approach requires additional processes for error compensation. When using optical square for squareness measurements, the occurrence of Abbe's offset is inevitable, which also leads to the generation of Abbe's error due to the combination of Abbe's offset with the angular error of the travel axis. During measurement, the space to install a straightness interferometer is limited due to the fixed position of the laser head, retro-reflector, and optical square. Thus, the effect of Abbe's error is increased. Also, limitations in the optics installation can cause difficulty in measuring the squareness along the full travel range.

In this study, a procedure to analyze the squareness measurement using a laser interferometer system is proposed to address concerns of a limited measurable range and the inevitable occurrence of Abbe's offset. The goals of this study are as follows:

(1) The elimination of Abbe's offset caused by optical square installation.

(2) The estimation of squareness for the full travel range using best fit methodology.

The analyzed results of the squareness measurement were evaluated by conducting experiments on the XY-plane of a three-axis machine tool using a laser interferometer system (XL-80, Renishaw plc, UK) and an optical square.

2. Measurement of Squareness using a Laser Interferometer System

2.1 Procedure for squareness measurement

Squareness can be calculated from two straightness data sets. First, the straightness of two axes should be measured under a common measurement coordinate. During the squareness measurement using a laser interferometer, the role of the optical square is to reflect the input laser beam by exactly 90 degrees.[20] The optical square is installed at the maximum measurable range of the axis, and then the laser head and straightness reflector (which are not included in the travel axis). Finally, straightness measurements are performed using the straightness interferometer along the direction of the travel axis. Similarly, the straightness measurement of another axis is carried out by moving the position of the interferometer only.

The measured straightness data are used in order to calculate the squareness about two axes, using the procedure-shown in Fig. 1. The straightness data (raw data) r_{yx}, measured in the horizontal direction (y-direction) of the X-axis includes Abbe's error due to the optical square setup and reference coordinate system setting. Therefore, the elimination of Abbe's error is required in this procedure. A representative line is determined from the straightness data m_{yx}, which is obtained after eliminating Abbe's error. Then we can find the inclination (α) of the

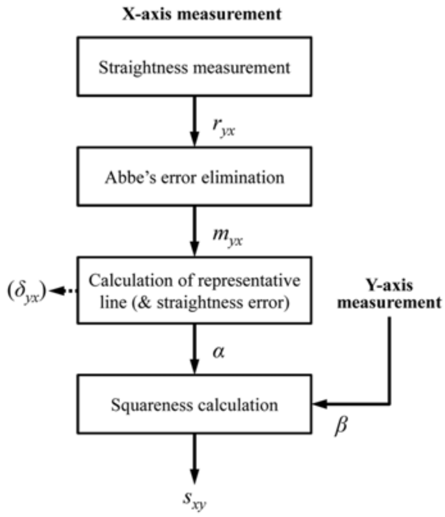

Fig. 1 Squareness evaluation procedure

straightness data with the X-axis. The inclination of the horizontal straightness of the Y-axis (β) is also calculated using a similar procedure. Finally, the squareness s_{xy} is calculated using the inclination of the straightness data of two axes, as described in the following Section 2.2.

2.2 Definition of representative line and squareness calculation

To calculate the squareness between two axes, a representative line from the straightness data must be defined. In the ISO230-1 standard, a definition for the representative line is introduced in two ways. The first method is to connect the two extreme end points of the data, and the other is defined using the least squares method as shown in Fig. 2(a).

For example, as shown in Eq. (1), the first method of drawing a representative line is realized by connecting the start point (x_0, $m(x_0)$) and end point (x_n, $m(x_n)$). The representative line using the least squares method is defined as the least squares line for which we minimize the sum of the squared error about all measurements as shown in Eq. (2). Thus,

$$y_{TP} = \frac{m(x_n) - m(x_0)}{x_n - x_0} x \tag{1}$$

$$y_{LS1} = a_0 + a_1 x \tag{2}$$

In order to define no straightness error at the origin, the method of least squares for the definition of a representative line was used without considering the constant term (intercept), as shown in Eq. (3):

$$y_{LS2} = a_1 x \tag{3}$$

The actual straightness error was obtained by eliminating the representative line from the Abbe's error-removed straightness measurement data, as shown in Eq. (4). This is shown graphically in Fig. 2(b). Thus,

$$\begin{aligned} \delta(x_i) &= m(x_i) - y_{TP}(x_i) \quad \text{for two extreme points} \\ \delta(x_i) &= m(x_i) - y_{LS}(x_i) \quad \text{for least squares} \end{aligned} \tag{4}$$

The inclinations of a representative line in the straightness data of the X-axis and Y-axis are α and β, respectively. Then, squareness s_{xy} is

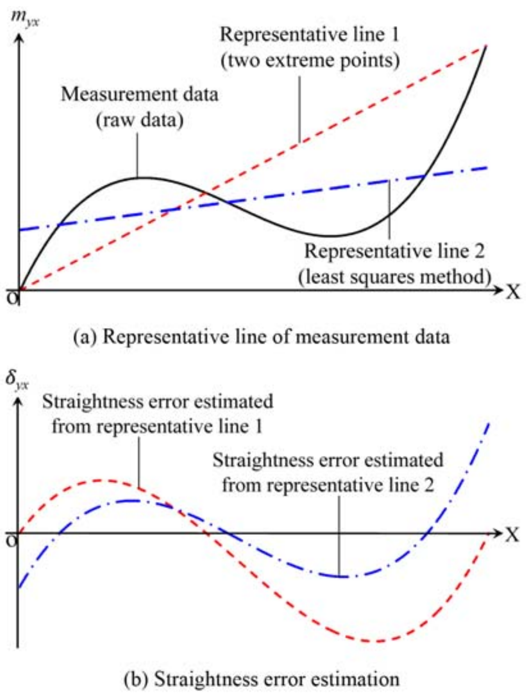

Fig. 2 Straightness error estimation using representative lines

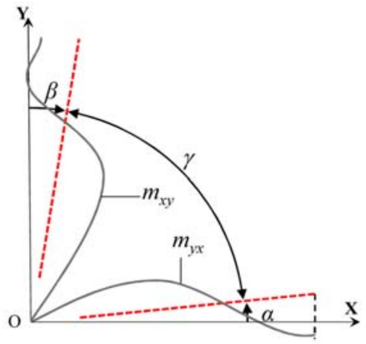

Fig. 3 Squareness and representative lines (y_{LS1} type) in the X-axis and Y-axis

calculated as the sum of the inclinations of the representative line, as shown in Eq. (5). Here, a negative sign for the squareness means it is less than 90 degrees, and a positive sign means it is greater than 90 degrees. The notation γ represents the angle between the two representative lines.

$$s_{xy} = \gamma - 90° = -(\alpha + \beta) \tag{5}$$

The relationship between two representative lines with the least squares method is shown in Fig. 3.

2.3 Abbe's error due to optical square setup

The occurrence of Abbe's offset can be avoided if the origin of the reference coordinate and the measurement coordinate of two axes coincide. However, when using an optical square for a squareness measurement, Abbe's offset is inevitable due to the constraint in the installation of optics in the machine tool. Abbe's offset depends on the reference coordinate system (RCS) of the machine tool, as shown in Fig. 4, and will always have at least two offset values. Abbe's offset is

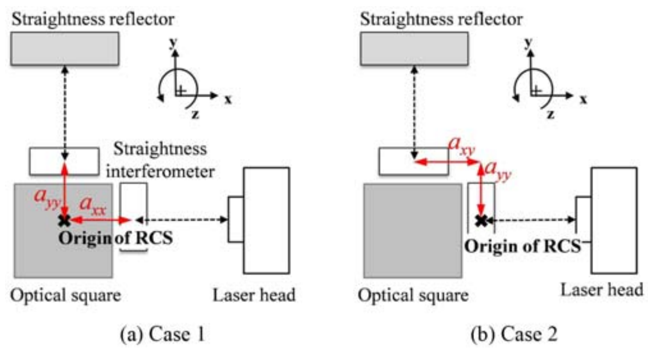

Fig. 4 Abbe's offset caused by optical square (a) Reference coordinate exists on the optical square (b) Reference coordinate exists on the straightness interferometer

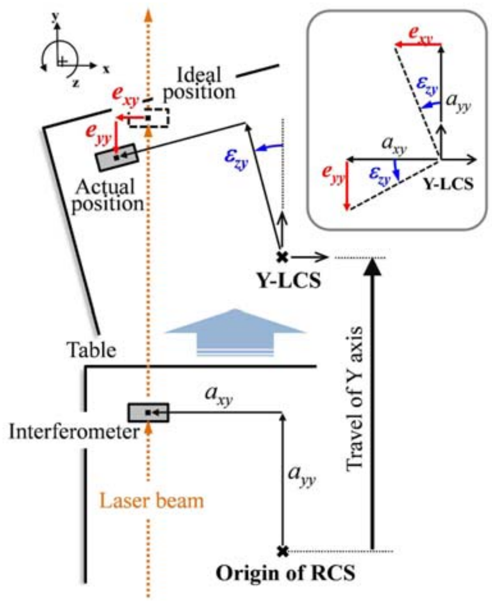

Fig. 5 Abbe's error due to positioning of interferometer

represented as a_{ij}, which means Abbe's offset in the i-direction of the j-axis.

These offsets affect the measurement data of geometric errors occurring in the traveling axis. For the measurement setup with reference coordinate as shown in Fig. 4(b), the Abbe's error (e_{xy}, e_{yy}) is caused by the two Abbe's offsets (a_{xy}, a_{yy}) combined with angular error ε_{zy} while traveling in the Y-axis with local coordinate system (Y-LCS), as shown in Fig. 5. These Abbe's errors are included both in the horizontal straightness measurement (m_{xy}) and linear displacement measurement (m_{yy}). Thus, the elimination of Abbe's error is an important step for error measurement during precision measurement, and is expressed as the following equation:

$$\mathbf{m}_j = \mathbf{r}_j - \mathbf{e}_j \tag{6}$$

where, $\mathbf{r}_j = [r_{xj} \; r_{yj} \; r_{zj}]$ and $\mathbf{e}_j = [e_{xj} \; e_{yj} \; e_{zj}]$ are the straightness measurement data with Abbe's offset and Abbe's error, respectively.

The occurrence of Abbe's error due to the Abbe's offset is presented using a kinematic chain as shown in Fig. 6 and a mathematical relation is developed. Here, each parameter is defined as a 4×4 matrix, as shown in Table 1. The homogeneous transformation matrix (HTM) representations

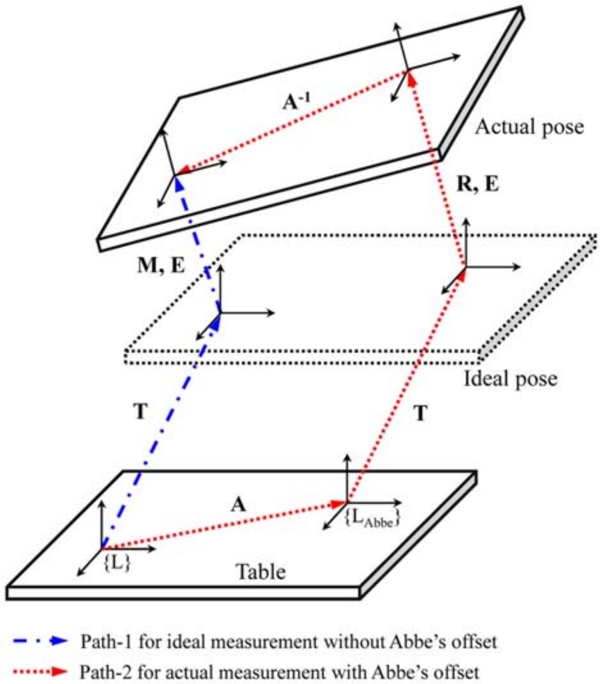

Fig. 6 Kinematic chain between the ideal and actual measurements

Table 1 Definition of geometric errors and motion parameters

Symbols	Description	Expression
A	Abbe's offset	$\begin{bmatrix} \mathbf{I} & \mathbf{a}_j \\ 0\,0\,0 & 1 \end{bmatrix}$
T	Machine instruction for the linear axis driving	$\begin{bmatrix} \mathbf{I} & \mathbf{t}_j \\ 0\,0\,0 & 1 \end{bmatrix}$
M	Straightness measurement without Abbe's offset	$\begin{bmatrix} \mathbf{I} & \mathbf{m}_j \\ 0\,0\,0 & 1 \end{bmatrix}$
R	Straightness measurement with Abbe's offset	$\begin{bmatrix} \mathbf{I} & \mathbf{r}_j \\ 0\,0\,0 & 1 \end{bmatrix}$
E	Angular error at the position of machine instruction	$\begin{bmatrix} \mathbf{I}+\mathbf{E}_j & \mathbf{0} \\ 0\,0\,0 & 1 \end{bmatrix}$

for path-1 (when the interferometer is setup without Abbe's offset) and path-2 (under the actual setup with Abbe's offset) are shown in Eqs. (7) and (8), respectively. Angular error $\mathbf{E}_j$ is given in Eq. (9).

$$\tau_1 = \mathbf{TME} \text{ (for path-1)} \quad (7)$$

$$\tau_2 = \mathbf{ATREA}^{-1} \text{ (for path-2)} \quad (8)$$

$$\mathbf{E}_j = \begin{bmatrix} 0 & -\varepsilon_{zj} & \varepsilon_{yj} \\ \varepsilon_{zj} & 0 & -\varepsilon_{xj} \\ -\varepsilon_{yj} & \varepsilon_{xj} & 0 \end{bmatrix} \quad (9)$$

In order to make a kinematic chain, the final HTMs of the two paths should be equal ($\tau_1 = \tau_2$). After the removal of high-order terms, the straightness without Abbe's error is obtained from the relationship as shown in Eq. (10).

$$\mathbf{m}_j = \mathbf{r}_j - \mathbf{E}_j\mathbf{a}_j \quad (10)$$

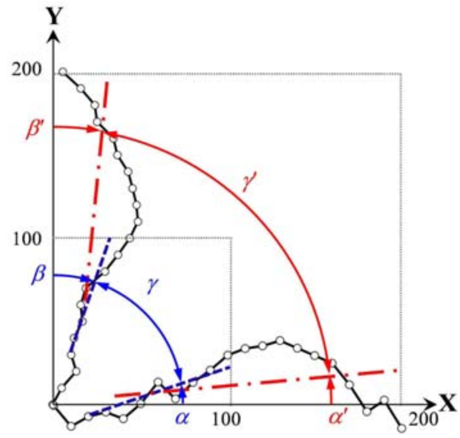

Fig. 7 Influence of travel range on the squareness measurement

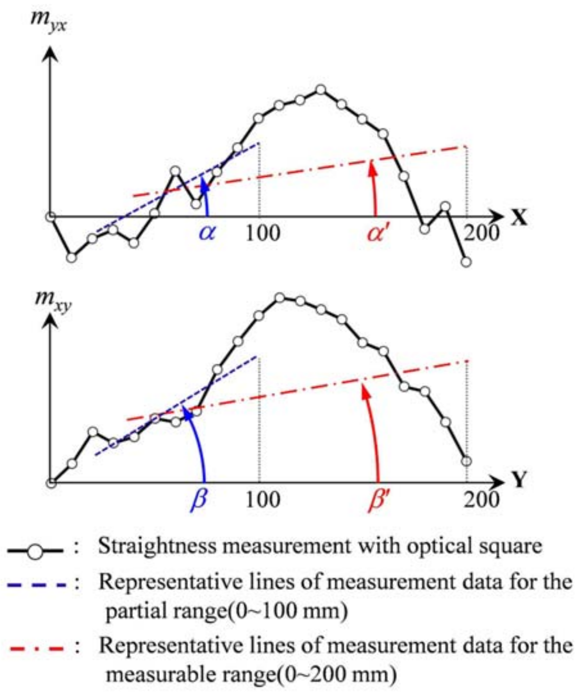

Fig. 8 Representative line according to the measurement range

Table 2 Difference of squareness results depending on measuring range

X (mm) × Y (mm)	α (μm/m)	β (μm/m)	s_{xy} (μm/m)
100×100	22.0	19.7	-41.7
200×200	6.0	5.5	-11.5

where, $\mathbf{a}_j = [a_{xj}\ a_{yj}\ a_{zj}]$ and $\mathbf{t}_j = [t_{xj}\ t_{yj}\ t_{zj}]$ are Abbe's offset and the machine instruction, respectively.

3. Estimation of Squareness for the Full Travel Range

3.1 Consideration of the measurement range

Generally, geometric error measurement and compensation are performed for the full travel range. However, for a squareness measurement using a laser interferometer, it is difficult to measure the squareness for the complete travel range due to constraints on the

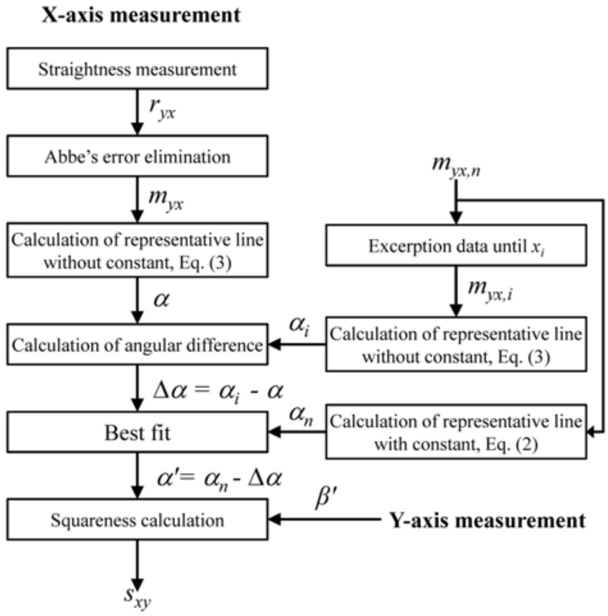

Fig. 9 Squareness evaluation procedure for the full travel range

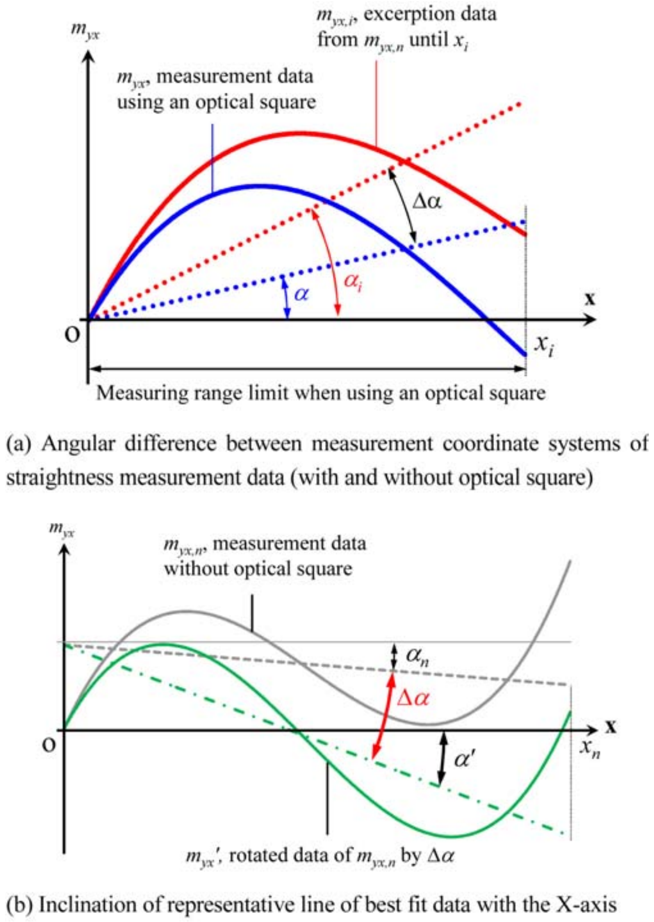

Fig. 10 Best fit of straightness measurement data for full range when using optical square

available space for the installation of an optical square, interferometer, and reflector. Obstacles such as the machine tool door and the outer cover are removed to avoid interference with the laser beam movement, and an additional fixture is required to install the optical square at a measurable position for the full range of the two axes.

Conducting the measurement over a partial range due to non-fulfillment of the extra demands poses a serious challenge to the exact measurement of the squareness. In our experiments using a laser interferometer system, the angle between the two representative lines for the partial range is γ, as shown in Fig. 7. Here, the partial range and inclination of the representative line (Fig. 8) with the X-axis and Y-axis are x_i, y_i, and α, β, respectively. Similarly, the inclinations of the representative line for the full travel range (x_n, y_n) are α' and β', respectively. The results of the two cases, as listed in Table 2, show that the measurement range critically affects the squareness value. Therefore, the squareness for the full range must be calculated using Eq. (11) instead of Eq. (5).

$$s_{xy} = \gamma' - 90° = -(\alpha' + \beta') \tag{11}$$

If straightness measurement data using an optical square are used in the commercial analysis program provided by the manufacturer, then squareness is analyzed only for the partial range and not for the full travel range. Therefore, in some cases, error compensation is performed using the opposite sign. Thus, in this study, a squareness estimation algorithm for the full travel range from the partial range data is proposed as shown in Fig. 9.

3.2 Best fit of straightness measurement data

For the straightness measurement of an independent axis, there is no need for the installation of an optical square, and thus the measurement can be easily performed for the full travel range. Also, the straightness of the full range with an optical square can be estimated using this data, as described below. When there is a coincidence of the two measurement coordinates, then the measured results of the aforementioned cases (with and without the optical square) will show the same result. Therefore, we propose a best-fit method for the estimation of straightness error for the full travel range when using an optical square.

We obtained different representative lines depending upon the measurement range. Therefore, squareness was not determined from the inclination α (partial range). Rather, it was determined from the inclination of a representative line about the full range α'. Thus, we can apply the additional procedure as shown in Fig. 9 by using the full range straightness data without an optical square for the squareness evaluation. Here, the data $m_{yx,i}$ are taken from the straightness data $m_{yx,n}$ measured about the full range without an optical square. The selected range is equivalent to the measurable range when using an optical square. Calculation of the inclination α_i of the representative line from the data $m_{yx,i}$ is followed by a new inclination α of the representative line of the estimated straightness for the full travel range using an optical square. For the best fit of two straightness measurements (Fig. 10(a)), inclination $\Delta\alpha$ is shown in Eq. (12). Here, inclinations α and α' are calculated using the representative line without the constant term from the data m_{yx}. Thus,

$$\Delta\alpha = \alpha_i - \alpha \tag{12}$$

If the straightness data without an optical square ($m_{yx,n}$) is rotated by the difference angle $\Delta\alpha$, then the straightness measurement for full

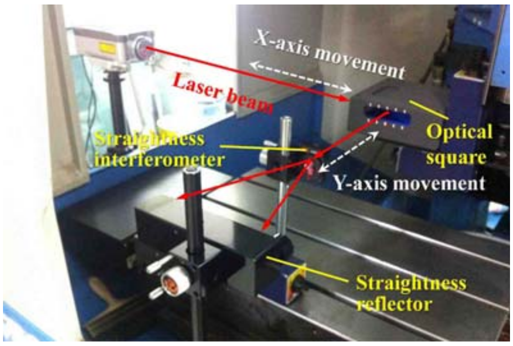

Fig. 11 Experimental setup for squareness measurement

Table 3 Specification for squareness measurement

Manufacturer	Renishaw plc, XL-80
Range	±3/M mm/m
Accuracy	±0.5% ±2.5 ±0.8M μm/m
Resolution	0.01 μm/m
M = measurement distance in meter of the longest axis % = percentage of the displayed value	

Table 4 Abbe's offset

	a_{xj} (mm)	a_{yj} (mm)	a_{zj} (mm)
X-axis	-538	8	0
Y-axis	-218	-308	0

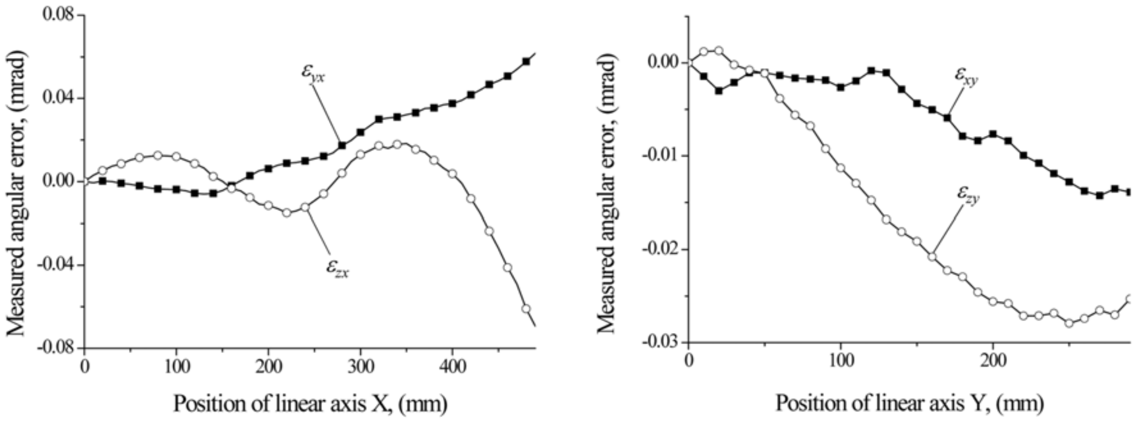

Fig. 12 Angular error measurements of (left) X-axis and (right) Y-axis

range straightness with an optical square is finally obtained as m_{yx} as shown in Fig. 10(b). Consequently, inclination of the representative line of the transformed straightness data α' was calculated as the difference between the inclination α_n (i.e., the representative line without an optical square), and the angular difference $\Delta\alpha$. Thus,

$$\alpha' = \alpha_n - \Delta\alpha \tag{13}$$

A similar procedure was applied to calculate the inclination angle β about the Y-axis as shown in Eq. (14). Finally, the squareness for the full travel range can be calculated using Eq. (11).

$$\beta' = \beta_n - \Delta\beta \tag{14}$$

4. Experiments

To confirm the effectiveness of the proposed procedure for the squareness analysis described in Section 3, a squareness measurement was performed for the XY-plane of a three-axis machine tool, as shown in Fig. 11. The measurement system consisted of a laser interferometer and optical square (XL-80, Renishaw plc, UK). Their specifications are shown in Table 3. In order to remove Abbe's error, angular error measurement (excluding roll error) was conducted three times for each axis with an interval of 10 mm, as shown in Fig. 12.

The installation space for the straightness interferometer was restricted due to the use of an optical square for measurement, which was installed near the spindle. Abbe's offset measured from the reference coordinate is shown in Table 4. The measurable ranges of the X-axis and Y-axis were restricted to 200 mm due to the optical square. The straightness measurement ranges of the X-axis and Y-axis without an optical square were 490 mm and 290 mm, respectively.

The results of the measured straightness and Abbe's error-removed straightness are shown in Fig. 13(a). It was necessary to eliminate the Abbe's error for precise measurement since there was a significant difference between the two straightness measurements. In order to estimate straightness when using the optical square for the full travel range by a best fit process, the inclination difference of two straightness representative lines (with and without the optical square) for a partial range (200 mm range) was calculated as shown in Fig. 13(b). The R-square value between the straightness data with an optical square and the transformed straightness data without an optical square for a 200 mm range is 92.78%. The estimated inclination α' of a representative line for the full travel range was calculated from the transformed straightness data, as shown in Fig. 13(c). Similarly, the inclination β' of the representative line was calculated for the Y-axis, as shown in Fig. 13 (right). Finally, the squareness for the full travel range was calculated from Eq. (12). Squareness results for the following three cases are compared in Table 5:

Case I: Commercial analysis software.

Case II: Proposed procedure along the partial travel range.

Case III: Proposed procedure along the full travel range.

The differences between results for Case I and II, and between II and III, are 4.3 μm/m and 33.55 μm/m, respectively. Abbe's error can have critically large value depending on the product outcome of Abbe's

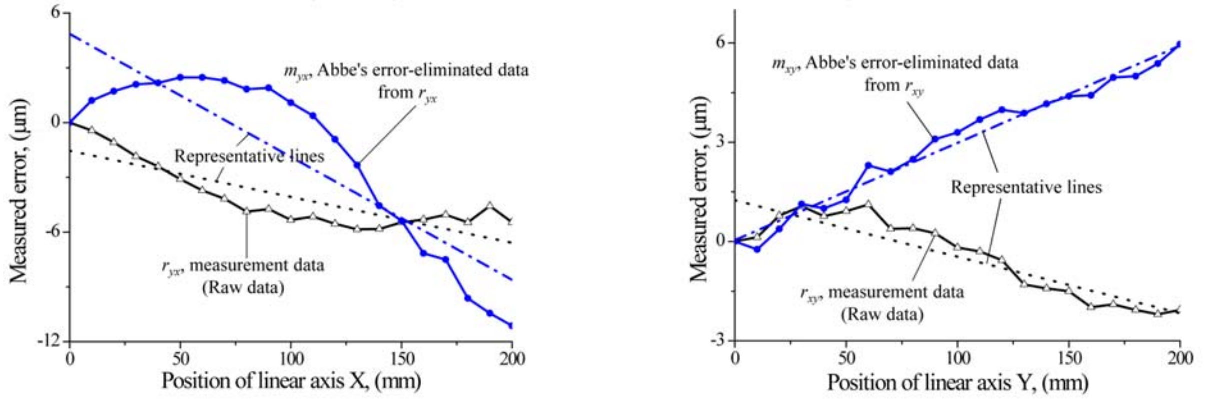

(a) Elimination of Abbe's error from measurement data

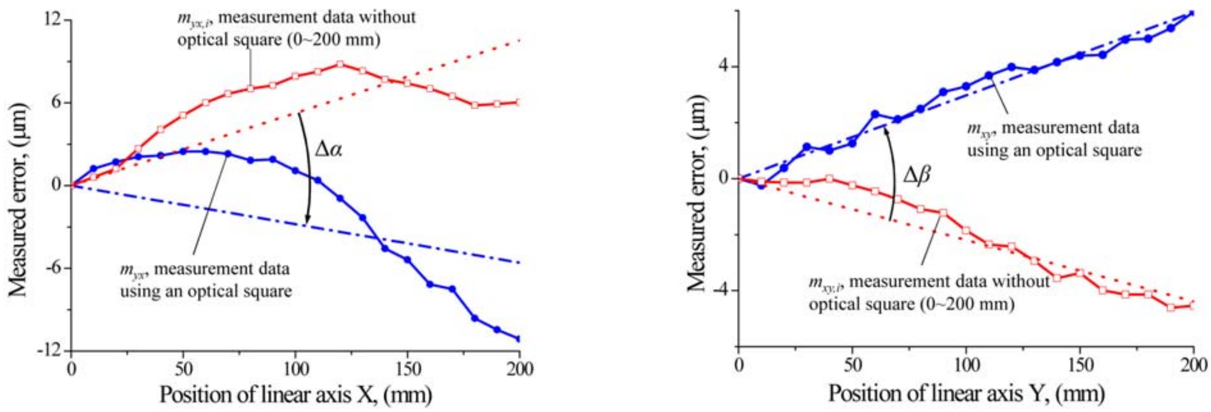

(b) Angular difference between measurement coordinate systems (with and without optical square)

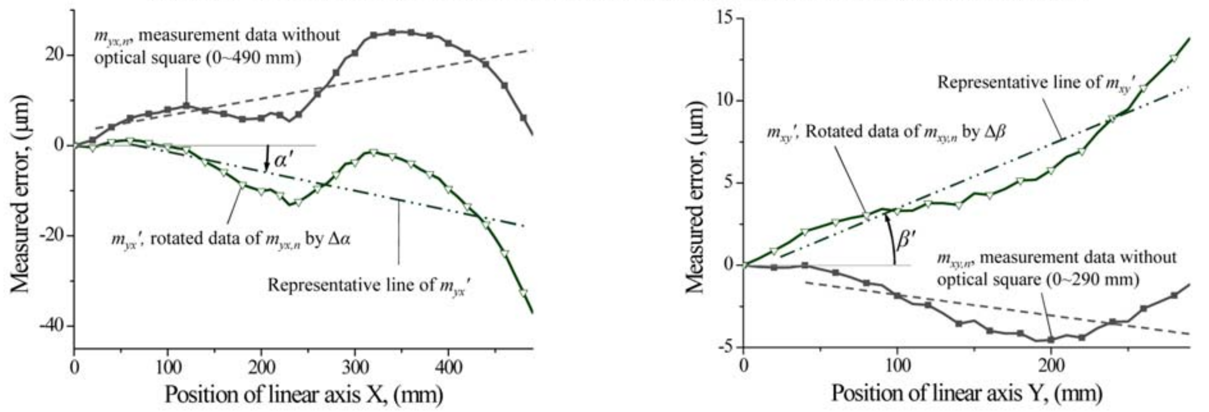

(c) Best fit of straightness data for the full travel range

Fig. 13 Abbe's error elimination and best fit of straightness measurement data (left) for X-axis and (right) Y-axis

Table 5 Results of squareness analysis

	Measurement range X (mm) × Y (mm)	Squareness (μm/m)
Case I	200×200	42.3
Case II	200×200	38.0
Case III	490×490	4.45

offset and angular error. Moreover the results (Case II, III) also showed squareness estimation critically depends on the measurement range. Thus squareness estimation without the elimination of Abbe's error and/or without the consideration for the full travel range results in undesired error compensation (usually followed by the present commercial software). For example, in some cases compensation is performed in the opposite direction due to incorrect sign of the measurement result.

Especially the measurable range constraint should be always considered in most of the measuring system for evaluating the squareness like when using a master square, DBB and so on.

5. Conclusion

In this study, problems during squareness measurements using a laser interferometer system with an optical square such as inevitable

Abbe's error and local squareness estimation due to the constrained measurable range are presented. A method is proposed for eliminating the Abbe's error and also for the squareness estimation by applying the best fit process to partial and full range data.

The proposed method highlights: (1) A generalized equation for the elimination of Abbe's error from the straightness errors using kinematic chain is developed and (2) The best fit process involves only simple subtraction of inclinations of representative lines of partial and full range data.

The proposed method improved the squareness measurement accuracy for the full travel range without the need for any modification in the existing machine tool setup.

ACKNOWLEDGEMENT

This work was supported by Priority Research Centers Program through the National Research Foundation of Korea (NRF) funded by the Ministry of Education (2010-0020089) and supported by Kyungpook National University Research Fund, 2012.

REFERENCES

1. Lee, J. H. and Yang, S. H., "Measurement of geometric errors in a miniaturized machine tool using capacitance sensors," Journal of Materials Processing Technology, Vol. 164-165, No. 0, pp. 1402-1409, 2005.

2. Yang, S., Yuan, J., and Ni, J., "Accuracy enhancement of a horizontal machining center by real-time error compensation," Journal of Manufacturing Systems, Vol. 15, No. 2, pp. 113-124, 1996.

3. Lee, D. M., Zhu, Z., Lee, K. I., and Yang, S. H., "Identification and measurement of geometric errors for a five-axis machine tool with a tilting head using a double ball-bar," Int. J. Precis. Eng. Manuf., Vol. 12, No. 2, pp. 337-343, 2011.

4. Lee, K. I., Lee, D. M., and Yang, S. H., "Parametric modeling and estimation of geometric errors for a rotary axis using double ball-bar," International Journal of Advanced Manufacturing Technology, Vol. 62, No. 5-8, pp. 741-750, 2012.

5. Schwenke, H., Knapp, W., Haitjema, H., Weckenmann, A., Schmitt, R., and Delbressine, F., "Geometric error measurement and compensation of machines-an update," CIRP Annals - Manufacturing Technology, Vol. 57, No. 2, pp. 660-675, 2008.

6. Lee, K .I., Lee, J. C., and Yang, S. H., "The Optimal Design of a Measurement System to Measure the Geometric Errors of Linear Axes," International Journal of Advanced Manufacturing Technology, Vol. 66, No. 1-4, pp. 141-149, 2013.

7. Lee, K. I. and Yang, S. H., "Robust Measurement Method and Uncertainty Analysis for Position-independent Geometric Errors of a Rotary Axis using a Double Ball-bar," Int. J. Precis. Eng. Manuf., Vol. 14, No. 2, pp. 231-239, 2013

8. Lee, K. I. and Yang, S. H., "Measurement and Verification of Position-independent Geometric Errors of a Five-axis Machine Tool using a Double Ball-bar," International Journal of Machine Tools and Manufacture, Vol. 70, pp. 45-52, 2013.

9. Yang, S. H., Kim, K. H., Park, Y. K., and Lee, S. G., "Error analysis and compensation for the volumetric errors of a vertical machining centre using a hemispherical helix ball bar test," International Journal of Advanced Manufacturing Technology, Vol. 23, No. 7-8, pp. 495-500, 2004.

10. ISO 230-1, "Test code for machine tools-Part 1: Geometric Accuracy of Machines Operating under No-load or Finishing Conditions," 1996.

11. Lee, C. W., Song, J. Y., and Ha, T. H., "Measurement of axis squareness by using reversal method," Proc. of the Korean Society of Precision Engineering Conference, pp. 445-448, 2005.

12. Hai, N., Yuan. J., and Ni. J., "Reverse Kinematic Analysis of Machine Tool Error using Telescoping Ball Bar," ASME Manufacturing science and engineering, pp. 277-286, 1994.

13. Lee, J. H., Liu, Y., and Yang, S. H., "Accuracy improvement of miniaturized machine tool: Geometric error modeling and compensation," International Journal of Machine Tools and Manufacture, Vol. 46, No. 12-13, pp. 1508-1516, 2006.

14. Lee, K. I., Lee, J. C., and Yang, S. H., "The optimal design of a measurement system to measure the geometric errors of linear axes," International Journal of Advanced Manufacturing Technology, Vol. 66, No. 1-4, pp. 141-149, 2013.

15. Chen, G., Yuan, J., and Ni, J., "A displacement measurement approach for machine geometric error assessment," International Journal of Machine Tools and Manufacture, Vol. 41, No. 1, pp. 149-161, 2001.

16. Castro, H. F. F. and Burdekin, M., "Dynamic calibration of the positioning accuracy of machine tools and coordinate measuring machines using a laser interferometer," International Journal of Machine Tools and Manufacture, Vol. 43, No. 9, pp. 947-954, 2003.

17. Agilent Technologies, "Agilent 5530 Laser Calibration System," pp. 12, 2012.

18. Renishaw plc., "Portable Laser Measurement and Calibration," pp. 15, 2011.

19. Steinmetz, C. R., "Sub-micron position measurement and control on precision machine tools with laser interferometry," Precision Engineering, Vol. 12, No. 1, pp. 12-24, 1990.

20. Renishaw plc, "Renishaw Laser Interferometer System Manual Ver. 2.1," 2009.